View metadata, citation and similar papers at core.ac.uk
brought to you by CORE
provided by Elsevier - Publisher Connector

FEBS Letters 583 (2009) 3593–3599

FEBS Letters
journal homepage: www.FEBSLetters.org

A locally-induced increase in intracellular Ca^{2+} propagates cell-to-cell in the presence of plasma membrane Ca^{2+} ATPase inhibitors in non-excitable cells

Tadashi Nakano [a,*], Takako Koujin [b], Tatsuya Suda [c], Yasushi Hiraoka [b,d,e], Tokuko Haraguchi [b,d,e]

[a] Frontier Research Base for Global Young Researchers, Frontier Research Center, Graduate School of Engineering, Osaka University, 2-1 Yamadaoka, Suita, Osaka 565-0871, Japan
[b] Kobe Advanced ICT Research Center, National Institute of Information and Communications Technology, 588-2 Iwaoka, Iwaoka-cho, Nishi-ku, Kobe 651-2492, Japan
[c] Department of Computer Science, Donald Bren School of Information and Computer Sciences, University of California, Irvine, CA 92697-3425, USA
[d] Graduate School of Frontier Biosciences, Osaka University, 1-3 Yamadaoka, Suita, Osaka 565-0871, Japan
[e] Graduate School of Science, Osaka University, 1-1 Machikaneyama, Toyonaka 560-0043, Japan

ARTICLE INFO

Article history:
Received 10 September 2009
Revised 5 October 2009
Accepted 12 October 2009
Available online 17 October 2009

Edited by Lukas Huber

Keywords:
Ca^{2+} signaling
Calcium-induced calcium release
Non-excitable cell
computational model

ABSTRACT

Intercellular Ca^{2+} waves are commonly observed in many cell types. In non-excitable cells, intercellular Ca^{2+} waves are mediated by gap junctional diffusion of a Ca^{2+} mobilizing messenger such as IP_3. Since Ca^{2+} is heavily buffered in the cytosolic environment, it has been hypothesized that the contribution of the diffusion of Ca^{2+} to intercellular Ca^{2+} waves is limited. Here, we report that in the presence of plasma membrane Ca^{2+} ATPase inhibitors, locally-released Ca^{2+} from the flash-photolysis of caged-Ca^{2+} appeared to induce further Ca^{2+} release and were propagated from one cell to another, indicating that Ca^{2+} was self-amplified to mediate intercellular Ca^{2+} waves. Our findings support the notion that non-excitable cells can establish a highly excitable medium to communicate local responses with distant cells.
© 2009 Federation of European Biochemical Societies. Published by Elsevier B.V. All rights reserved.

1. Introduction

Calcium ions (or Ca^{2+}) are ubiquitous second messengers that regulate a large number of cellular processes in virtually all mammalian cells. In electrically excitable cells such as cardiac and smooth muscle cells, Ca^{2+} propagates from cell-to-cell via gap junction channels. Known as intercellular Ca^{2+} waves, this form of communication provides a means by which adjacent cells coordinate their behavior. A major mechanism underlying intercellular Ca^{2+} waves in excitable cells is calcium-induced calcium release (CICR) [1], which amplifies Ca^{2+} through ryanodine receptors (RyRs). In electrically non-excitable cells such as epithelial cells, on the other hand, functional RyRs are rarely or only weakly expressed [2]. In such cases, Ca^{2+} itself propagates poorly between cells, and is affected by Ca^{2+} clearance mechanisms and buffering effects in the cytosol [3,4]. In non-excitable cells, a different mechanism of intercellular Ca^{2+} waves is more commonly found in which Ca^{2+} mobilizing molecules such as IP_3 rather than Ca^{2+} diffuse through gap junction channels intercellularly to activate IP_3 receptors that release Ca^{2+} [5,6].

In this paper, we demonstrate using non-excitable cells that a locally-induced Ca^{2+} increase propagated cell-to-cell via a CICR-like mechanism presumably without IP_3 diffusion when a Ca^{2+} clearance mechanism (plasma membrane Ca^{2+} ATPase: PMCA) was inhibited by sodium orthovanadate. This indicates that Ca^{2+} was self-amplified to mediate the propagation of intercellular Ca^{2+} waves in non-excitable cells. We also show through the use of a computational model that the experimentally observed effects of PMCA inhibition on intercellular Ca^{2+} wave propagation were in good agreement with computer simulation results.

2. Materials and methods

2.1. Materials

A PMCA inhibitor, sodium orthovanadate [7] was purchased from Sigma and dissolved in water. Another PMCA inhibitor, 5-(and-6)-carboxyeosin [8] was purchased from Invitrogen and dissolved in DMSO.

2.2. Cell culture

HeLa cells constitutively expressing connexin 43 (Cx43, designated HeLa Cx43 cells) (a gift from Dr. K. Willecke of Institut für

Abbreviations: PMCA, plasma membrane Ca^{2+} ATPase; CICR, calcium-induced calcium release; Cx43, connexin 43; $[Ca^{2+}]_i$, cytosolic calcium concentration

* Corresponding author. Fax: +81 6 6879 7199.
E-mail address: tnakano@wakate.frc.eng.osaka-u.ac.jp (T. Nakano).

0014-5793/$36.00 © 2009 Federation of European Biochemical Societies. Published by Elsevier B.V. All rights reserved.
doi:10.1016/j.febslet.2009.10.032

Genetik, Germany) [9] were cultured in Dulbecco's Modified Eagle Medium (DMEM) supplemented with 10% fetal calf serum (Gibco), 100 i.u./mL penicillin and 100 μg/mL streptomycin (Sigma). The cells were incubated in 10 cm diameter culture dishes at 37 °C under 5% CO_2. Prior to flash-photolysis experiments, cells were transferred to 35 mm glass-bottom dishes and cultured for 1–3 days under the same culture conditions.

2.3. Immunofluorescence analysis

The primary antibody used in the immunofluorescence analysis was anti-Cx43 mouse monoclonal antibody (Chemicon; human Cx43 detected), and the secondary antibody was Alexa 488-conjugatedgoat anti-mouse IgG (Molecular Probes).

2.4. Microinjection of Lucifer Yellow

Cells were microinjected with Lucifer Yellow (Molecular Probes) as a 4% solution in distilled water. Lucifer Yellow (MW = 443) is capable of propagating from cell-to-cell in the presence of functional gap junction channels. For fluorescence imaging of Lucifer Yellow, 430/528 nm wavelengths were used for excitation/emission, and fluorescence images were obtained 3–5 min after microinjection.

2.5. Fluo-4 and caged-Ca^{2+} loading

Cytosolic calcium concentrations ($[Ca^{2+}]_i$) were monitored using the calcium indicator, Fluo4/AM (Molecular Probes). Cells were first loaded with 2.0 μM Fluo4/AM in Hank's balanced salt solution buffered with 25 mM *N*-2-hydroxyethylpiperazine-*N*′-2-ethanesulfonic acid containing Ca^{2+} [HBSS-HEPES (+)] for 40 min at room temperature. The cells were subsequently loaded with 2.5 μM caged-Ca^{2+} (o-nitrophenynl EGTA, AM) (Invitrogen) for 10 min at room temperature. Cells were then washed twice with the HBSS-HEPES (+) and were left for 20 min prior to flash-photolysis experiments to allow for de-esterification of the AM esters.

2.6. Flash-photolysis of caged-Ca^{2+} and Ca^{2+} imaging

Flash-photolysis of caged-Ca^{2+} and Ca^{2+} imaging were performed using a fluorescence microscope system (DeltaVision, Applied Precision Inc., Seattle, WA) equipped with a 406 nm diode laser module (30 mW). In flash-photolysis experiments, Ca^{2+} was photo-released by laser spot illumination (excitation wavelength 406 nm). The center of a cell was selected and the selected spot was exposed for 1.0 s. Before and after the Ca^{2+} photo-release event, $[Ca^{2+}]_i$ was determined by the fluorescence intensity of Fluo4 at 488/528 nm wavelengths for excitation/emission. Fluorescence images were obtained using a 40, 60, or 100× oil lens objective with a 0.2–1.0 s image time interval. Cytosolic Ca^{2+} concentrations in figures are expressed as relative fluorescence intensity; i.e., $(F_t - F_0)/F_0$, where F_t is the fluorescence intensity measured at time t after the flash is applied and F_0 the resting fluorescence intensity measured prior to the flash. Control experiments were performed with Fluo4 but without loaded caged-Ca^{2+} to confirm that applying the flash itself had no effect on $[Ca^{2+}]_i$.

2.7. Mathematical modeling

A classical model of Ca^{2+} oscillation [10] is used to identify conditions under which Ca^{2+} propagates in a self-amplifying manner. In brief, $[Ca^{2+}]_i$ is represented as Z and that of the calcium store is Y. The time evolution of Z and Y is described by Eqs. (1) and (2), respectively, where v_0 represents Ca^{2+} influx from the extracellular environment to the cytosol, v_1 and v_2 represent Ca^{2+} uptake to and release from the calcium store, respectively, k_fY is the Ca^{2+} leak from the calcium store to the cytosol, and kZ represents Ca^{2+} actively transported from the cytosol to the extracellular environment by PMCA pumps. v_1 and v_2 are further described in Eqs. (3) and (4), respectively, using rate constants (V_{M1}, V_{M2}), threshold constants (K_1, K_R, K_A) and Hill coefficients (n,m,p).

$$\frac{dZ}{dt} = v_0 - v_1 + v_2 + k_fY - kZ \tag{1}$$

$$\frac{dY}{dt} = v_1 - v_2 - k_fY \tag{2}$$

$$v_1 = V_{M1}\frac{Z^n}{K_1^n + Z^n} \tag{3}$$

$$v_2 = V_{M2}\frac{Y^m}{K_R^m + Y^m}\cdot\frac{Z^p}{K_A^p + Z^p} \tag{4}$$

To simulate intercellular propagation of a locally-induced Ca^{2+} increase, the model was spatially extended to a one dimensional array of cells, where each cell is represented as Z_i and Y_i ($i = 0$ to $N-1$): N is the number of cells tested. The intercellular Ca^{2+} flux to Z_i is defined as $D/L^2\cdot(Z_{i-1} - 2Z_i + Z_{i+1})$, where D is the diffusion coefficient of Ca^{2+} and L is the size of the array. To simulate a Ca^{2+} photo-release event within a cell, v_f was added to dZ_0/dt for the first T s.

All simulation results were obtained by numerically integrating the model equations using Euler's method with a 0.0001 s time step. The parameter k is the Ca^{2+} extrusion rate constant controlled by PMCA pumps and is varied to observe its impact on the propagation of intercellular Ca^{2+} waves. The other parameter values used are as follows: $v_0 = 0.2$ (μM/s), $k_f = 0.2$ (1/s), $V_{M1} = 10$ (μM/s), $V_{M2} = 100$ (μM/s), $K_1 = 1$ (μM), $K_R = 2$ (μM), $K_A = 0.9$ (μM), $m = n = 2$, $p = 4$, $N = 30$ (cells), $v_x = 0.3$ (μM/s), $D = 20$ (μm/s^2), $L = 20$ (μm), and $T = 1.0$ (s).

3. Results

3.1. Functional gap junction channels are formed between HeLa Cx43 cells

The gap junction is a potential gate for Ca^{2+} propagation in many mammalian cells. To investigate whether gap junction channels exist in HeLa Cx43 cells, we first examined the localization of Cx43 in HeLa Cx43 cells by indirect immunofluorescence staining. The specific antibody localized Cx43 clustering at cell boundaries as expected for the gap junction (Fig. 1A). Second, we examined if the gap junction channels were functional by monitoring the diffusion of microinjected Lucifer Yellow, a membrane-impermeable tracer, to neighboring cells through the gap junction channels (Fig. 1B). The gap junction channel-forming rate (a coupling rate) was calculated as a ratio of the number of cells that increased their fluorescence intensity out of the number of cells adjacent to the Lucifer Yellow-injected cell. The average coupling rate of the HeLa Cx43 cells from our experiments was 0.39 ± 0.1 ($n = 56$), which is in good agreement with a previously reported value [9]. These results suggest that HeLa Cx43 cells form gap junctions with functional channels capable of propagating small molecules such as Ca^{2+}.

3.2. No apparent cell-to-cell propagation of calcium

To determine whether Ca^{2+} propagates through gap junction channels in HeLa Cx43 cells, two sets of experiments (Expts. 1 and 2) were performed using flash-photolysis of caged-Ca^{2+}. In Expt. 1, a flash was applied for 1.0 s to individual cells that had no physical contact with other cells (Fig. 2A). In Expt. 2, a flash was applied for the same duration to cells that were physically touching 3–6 other cells (Fig. 2B). In both cases, flashed cells exhib-

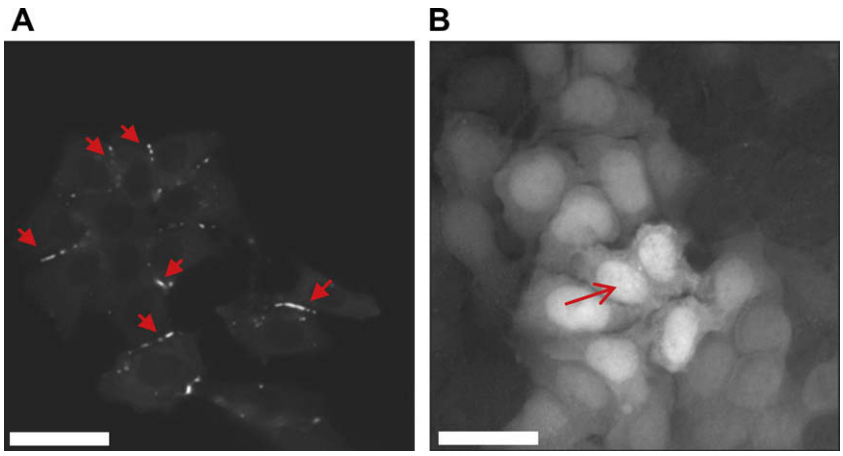

Fig. 1. Cx43 expression and gap junction channel formation. (A) Immunofluorescence analysis of Cx43 detected the localization of fluorescence along the boundary between two adjacent cells. The arrows point to strong fluorescence intensity (scale bar: 20 μm). (B) Gap junction channel formation was assayed by microinjection of Lucifer Yellow. Lucifer Yellow was injected to the cell marked with the arrow and spread to all adjacent cells (scale bar: 20 μm).

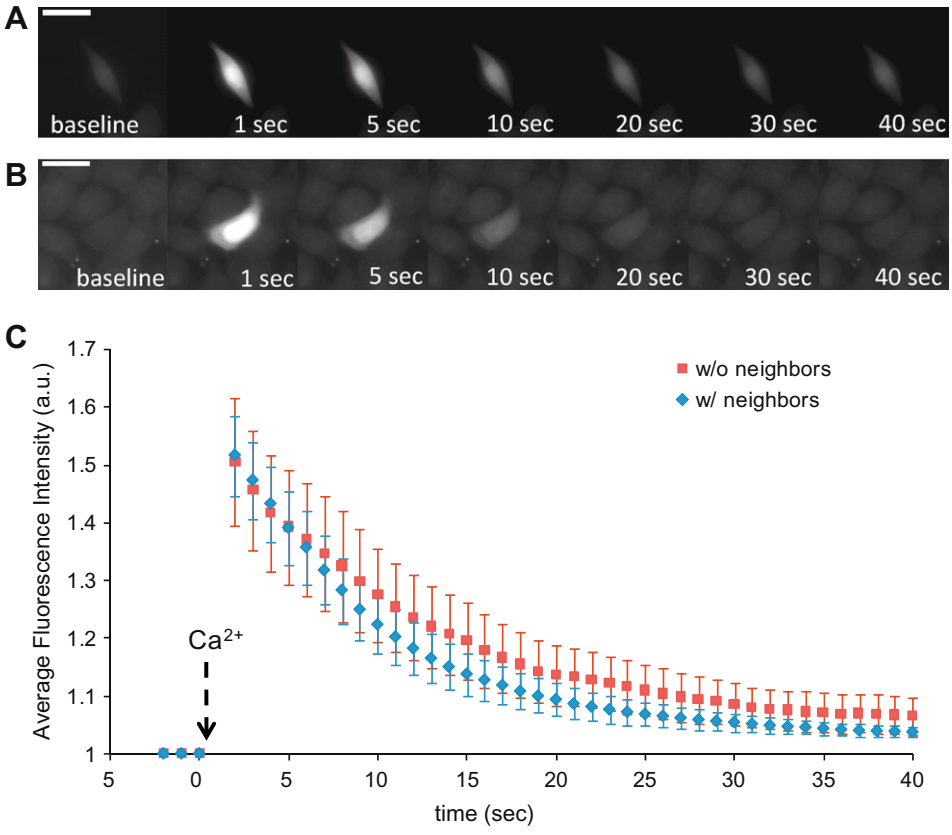

Fig. 2. Flash-photolysis of caged-Ca^{2+} under control conditions. (A and B) Each image sequence shows a series of Fluo4 fluorescence images obtained before (baseline) and after a 1.0 s flash was applied to the center of a cell at time 0. (A) The flashed cell is not in contact with other cells. (B) The flashed cell is in physical contact with other cells. (C) The Fluo4 fluorescence intensity averaged over the entire cytosolic region of a flashed cell is plotted for Expt. 1 (without neighboring cells, e.g., (A)) and Expt. 2 (with neighboring cells, e.g., (B)). The fluorescence intensity shown is relative to the baseline intensity. The increased decay rate in Expt. 2 indicates that Ca^{2+} diffuses between cells, although an increase in $[Ca^{2+}]$ was rarely observed with Fluo4 imaging in cells adjacent to a flashed cell (scale bar: 20 μm).

ited an increased $[Ca^{2+}]_i$ (Fluo4 fluorescence intensity averaged over the cytosolic region) upon photo-release of Ca^{2+}, which then gradually decreased (Fig. 2C). The average peak amplitudes measured in Expts. 1 and 2 were 1.50 ± 0.13 (n = 15) and 1.49 ± 0.07 (n = 19), respectively, for which the results were not significantly different. On the other hand, the average decay half-time, 9.93 ± 0.79 s (n = 15) for isolated cells (Expt. 1), was slightly higher than that for injected cells surrounded by other cells (7.52 ± 1.09 s (n = 19)) (Expt. 2, $P < 0.05$). As it is evident that gap junctions are formed in approximately 40% of cells (see above), this slightly accelerated decay could be indicative of the diffusion of Ca^{2+} through gap junction channels, even though an increase in $[Ca^{2+}]_i$ was rarely observed in Expt. 2. Since a significant decrease in $[Ca^{2+}]_i$ occurred both in Expts. 1 and 2, irrespective of the presence

or absence of neighboring cells, we speculated that this decrease could be caused by mechanisms other than diffusion through gap junctions. One such mechanism could involve PMCA pumps which have been reported to control the intracellular Ca^2 concentration in neurons [11].

3.3. PMCA inhibitors increase the intracellular calcium concentration

To test our hypothesis that PMCA pumps may act on controlling intracellular Ca^2 concentration in HeLa Cx43 cells, we used sodium orthovanadate, a known PMCA inhibitor [7], to reduce the effects of PMCA that transports Ca^{2+} to the extracellular environment, thereby enabling Ca^{2+} in the cytosolic region to extend their effective range of action.

The effects of PMCA inhibition on resting $[Ca^{2+}]_i$ were examined with different concentrations of sodium orthovanadate: high (2 mM), medium (500 μM) and low (50 μM). Under all conditions tested, PMCA inhibitor had a certain effect, but classified into three different types, on the Ca^{2+} dynamics in the cells, suggesting that PMCA pumps might act on controlling intracellular Ca^{2+} in the cells. For each concentration used, the Ca^{2+} dynamics of each cell in the presence of sodium orthovanadate was characterized into following three types as a large increase (Fig. 3A and D-1), an oscillatory response (Fig. 3B and D-2), or a small increase (Fig. 3C and D-3). A large increase was most often observed in the presence of the high concentration of sodium orthovanadate (2 mM) ($n = 4$), the oscillatory response in the presence of the medium concentration (500 μM) ($n = 4$), and small increases when cells were exposed to low concentrations (50 μM) ($n = 4$) (Fig. 3E).

3.4. Low concentrations of PMCA inhibitors caused a locally-induced increase of intracellular calcium which propagated from cell-to-cell

To assess the ability of a Ca^{2+} increase to propagate cell-to-cell in the presence of sodium orthovanadate, we used a low concentration of sodium orthovanadate that had almost no observable effects on resting $[Ca^{2+}]_i$ or only slightly increased it. Flash-photolysis experiments were performed under conditions where the resting $[Ca^{2+}]_i$ was slightly increased in the presence of sodium orthovanadate, with results showing that a local $[Ca^{2+}]_i$ increase induced by the flash-photolysis was propagated to adjacent cells. We observed increased $[Ca^{2+}]_i$ as far as five cells away from the flashed cell (Fig. 4A and B), with the increased $[Ca^{2+}]_i$ propagating a distance of 2.2 ± 0.4 cells ($n = 10$; excluding the flashed cell) on average. The amplitude of the Ca^{2+} transiently observed in an adjacent cell was sometimes equal to or greater than that in the flashed cell, indicating that further Ca^{2+} release was seemingly triggered in adjacent cells. (See Supplementary Fig. S1 for averaged amplitudes and time delay in Ca^{2+} increases between two adjacent cells.)

The PMCA inhibitor, sodium orthovanadate, used in the above experiments is a general ATPase inhibitor. To verify the effect of PMCA inhibition, we also used 5-(and-6)-carboxyeosin (CE), a more specific PMCA inhibitor [8]. Similar to the results of experiments using sodium orthovanadate, low concentrations (10 μM) of CE did not cause significant changes to the resting $[Ca^{2+}]_i$, inducing only slight increases or small amplitude, low frequency oscillations. In flash-photolysis experiments performed with low concentrations of CE, a locally-induced Ca^{2+} increase in the flashed cell

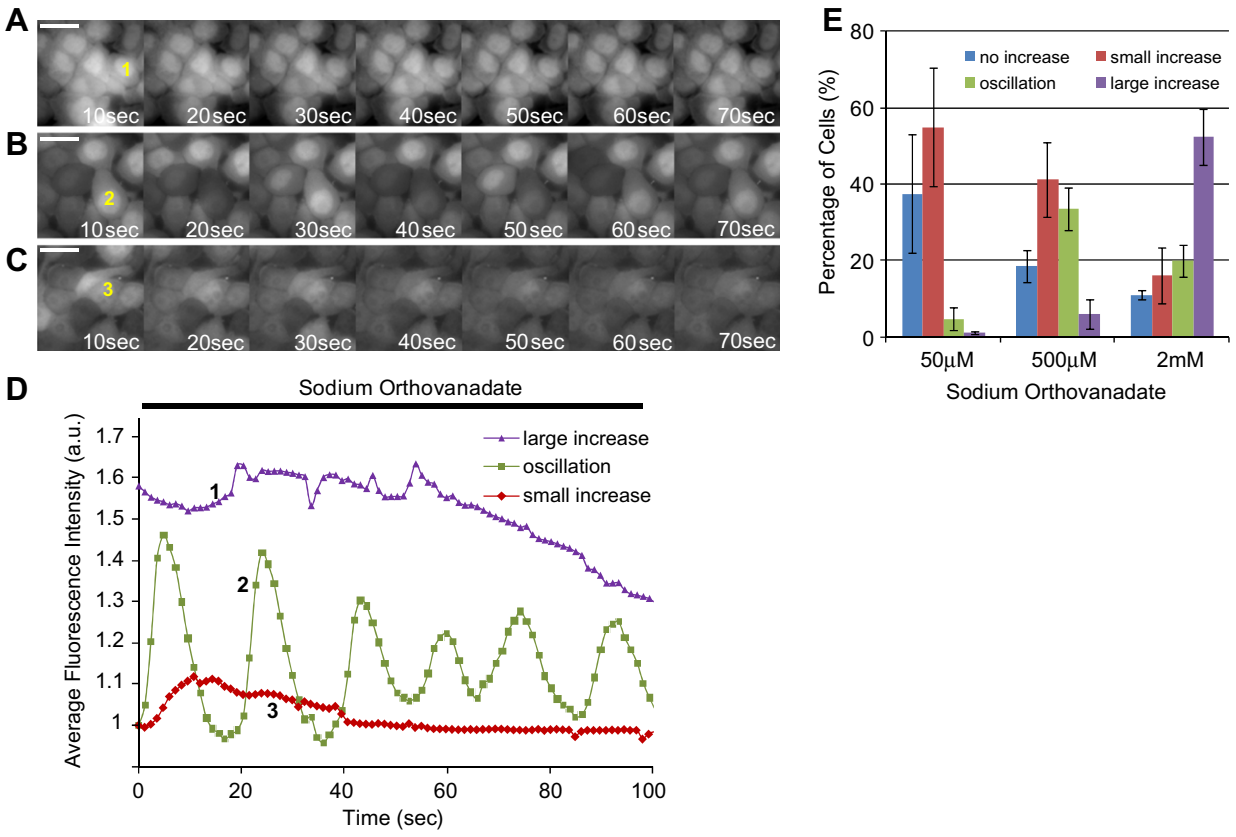

Fig. 3. Effects of sodium orthovanadate on Ca^{2+} dynamics. (A–C) The Ca^{2+} dynamics in response to the addition of sodium orthovanadate fall into three distinct patterns; a large increase (A), oscillation (B), small increase (C), (and no observable change with Fluo4 imaging). (D) The three traces show the average Fluo4 fluorescence intensity of three selected cells from (A–C), each representing one of the three forms of Ca^{2+} dynamics. The three cells are selected from (A–C) and indicated by numbers. (E) A large increase was observed mostly following exposure to high concentrations of sodium orthovanadate (2 mM), oscillatory responses upon exposure to medium concentrations (500 μM), and small increases in response to low concentrations (50 μM).

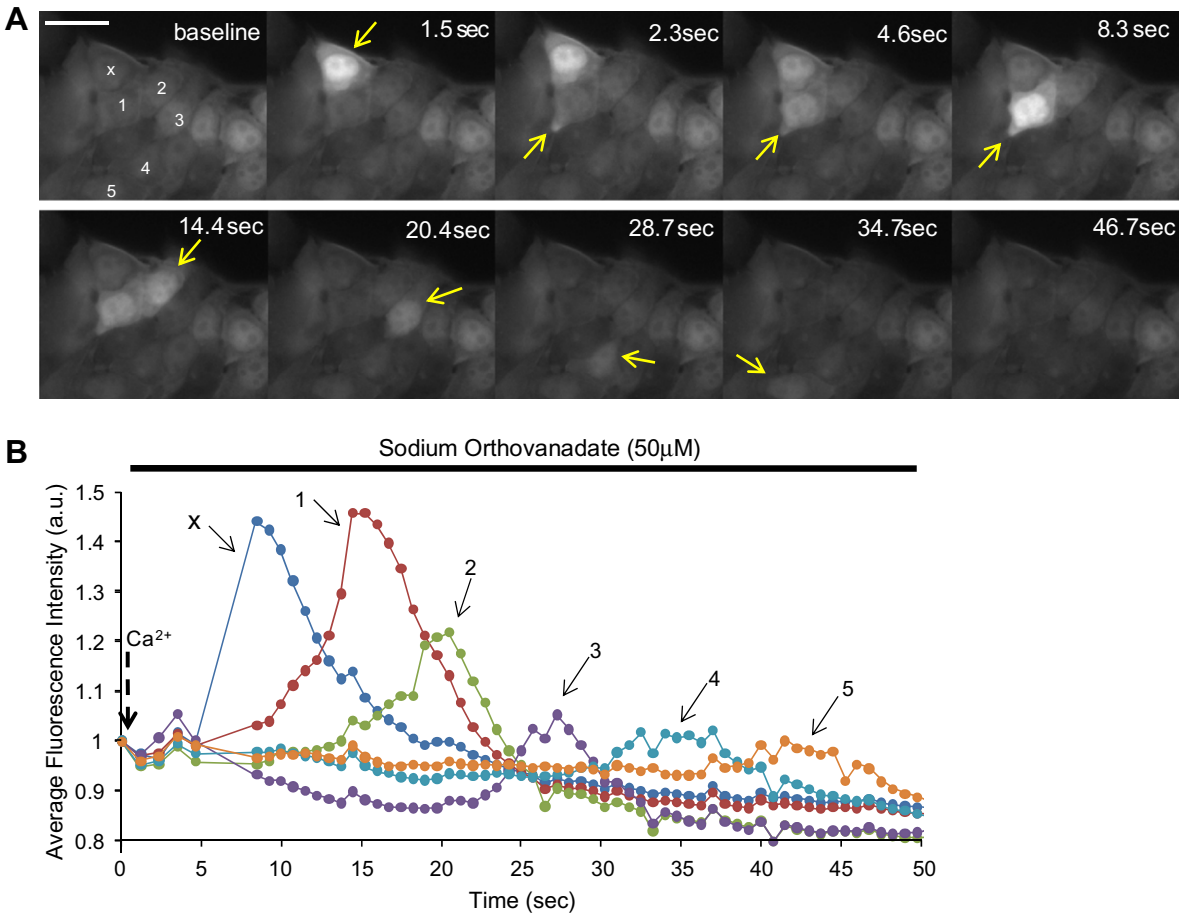

Fig. 4. Flash-photolysis of caged-Ca^{2+} in the presence of sodium orthovanadate (50 μM) induced an intercellular calcium wave that propagated cell-to-cell. (A movie is available online as supplementary data.) (A) Cell x increased its $[Ca^{2+}]_i$ and subsequently cells 1, 2, 3, 4 and 5 increased their $[Ca^{2+}]_i$. The arrows point in each case to the cell showing increased $[Ca^{2+}]_i$. (B) Traces of the average Fluo4 fluorescence intensity measured for each of the six cells.

propagated to adjacent cells. The average propagation distance measured was 1.7 ± 0.4 cells (n = 12).

3.5. Experimentally observed effects of PMCA inhibitors on intercellular Ca^{2+} propagation were in good agreement with theoretical results

To understand effects of PMCA inhibitors on intercellular Ca^{2+} propagation, we applied a mathematical model to simulate these phenomena as described in Methods. The experimentally observed effects of PMCA inhibitors on intercellular Ca^{2+} propagation were in good agreement with theoretical results obtained from a modified version of the classical model of calcium oscillation in non-excitable cells [10]. Fig. 5A illustrates the model used in this study in which the Ca^{2+} extrusion rate constant (k) represents PMCA activities (larger k values indicate that PMCA pumps are more active or less inhibited). Fig. 5B shows simulation results demonstrating how the PMCA Ca^{2+} extrusion rate constant (k) impacts the Ca^{2+} dynamics. The resting $[Ca^{2+}]_i$ is low for a high Ca^{2+} extrusion rate (k = 0.70), oscillates for an intermediate Ca^{2+} extrusion rate (k = 0.60), and is sustained at a high level for a low Ca^{2+} extrusion rate (k = 0.28). The simulation results here are thus in good agreement with the experimental results shown in Fig. 3D.

Fig. 5C shows the distance that a locally-induced Ca^{2+} increase propagates along an array of cells for a range of k values. When k is large, a locally-induced Ca^{2+} increase does not propagate (no propagation). When k is reduced, the Ca^{2+} increase propagates along the array, but is attenuated as it proceeds (diffusion-like propagation). When k is reduced even further, a locally-induced Ca^{2+} increase propagates in a self-amplifying manner to the end of the cell array (regenerative propagation). (It is therefore in theory possible that a Ca^{2+} increase propagates from a flashed cell to all the other cells, however, such a case was not observed in our experiments due, for instance, to the fact that the gap junction channel-forming rate was about 40% and channels were not always formed.) The experimental results shown in Fig. 4B can be well reproduced when the PMCA Ca^{2+} extrusion rate constant is small (k = 0.723) as shown in Fig. 5D. It is noted here that similar observations can be made for other model parameters. For example, increasing the rate for v_0 and v_2, and decreasing the rate for v_1 has a similar effect as decreasing k, which allows a locally-induced Ca^{2+} increase to propagate cell-to-cell.

4. Discussion

Previous studies based on non-excitable cells [12–14] show that a local Ca^{2+} increase induced by either microinjection of Ca^{2+} or flash-photolysis of caged-Ca^{2+} was able to generate a Ca^{2+} wave that propagated cell-to-cell through a CICR-like mechanism after cells were stimulated with agonists. Since agonistic stimulation is known to produce IP_3, it has been hypothesized that an elevation of the basal IP_3 level (or the supra-basal IP_3 level) is required to activate such a self-amplifying mechanism in non-excitable cells.

In our experiments, we used PMCA inhibitors, which are not known to produce IP_3, and demonstrated that a locally-induced in-

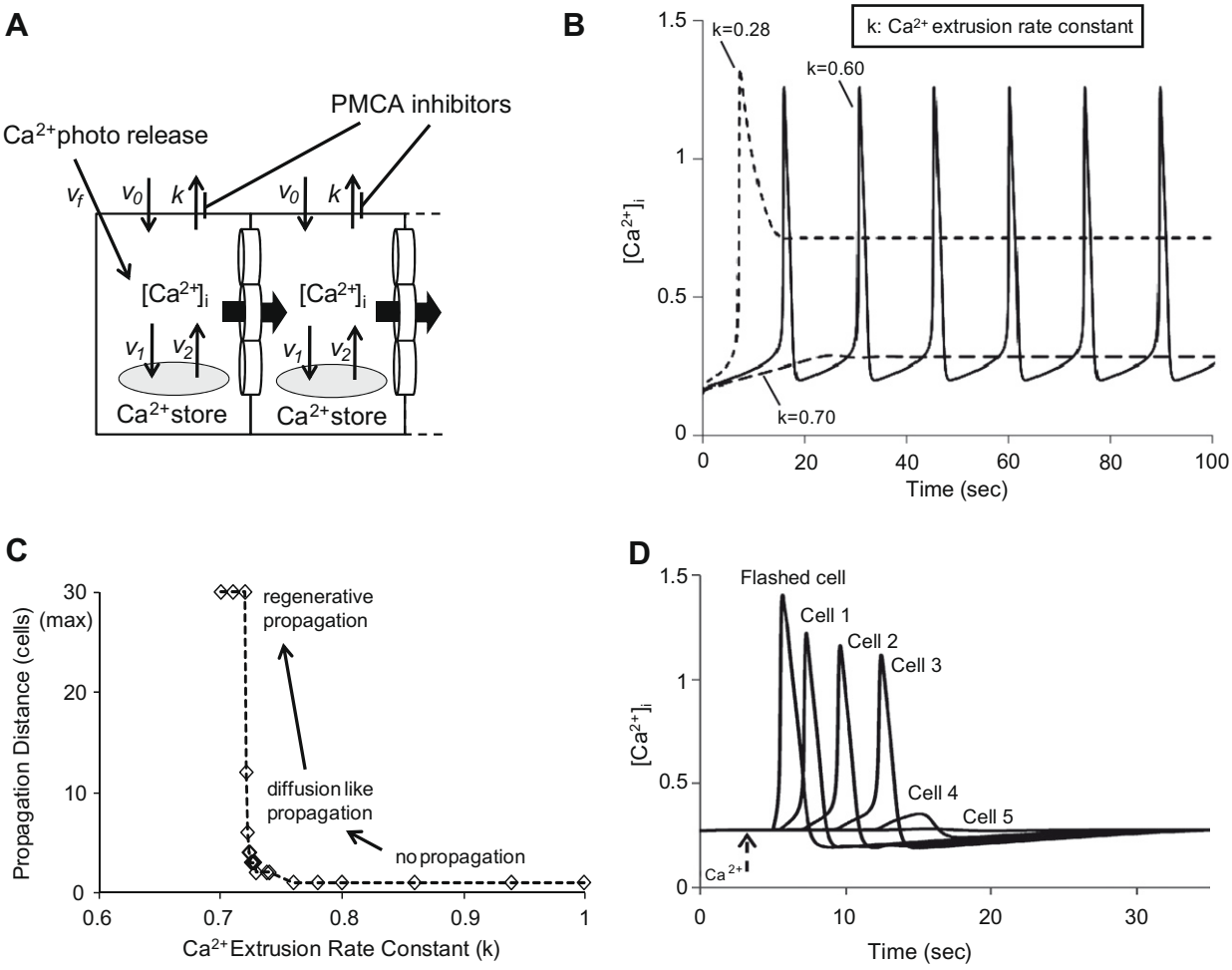

Fig. 5. Theoretical results supporting experimentally observed effects of plasma membrane Ca^{2+} ATPase (PMCA) inhibitors. (A) The model used in the theoretical study is shown (Only selected parameters are shown.). Model parameter *k* represents the Ca^{2+} extrusion rate constant, which is affected by PMCA inhibition. (B) The simulation studies investigated the impact of PMCA inhibition on $[Ca^{2+}]_i$ dynamics, and show good agreement with the experimental results in Fig. 3D. (C) The simulation studies investigated the impact of PMCA inhibition on the distance that a locally-induced Ca^{2+} increase can propagate. (D) The simulation results obtained from a specific *k* value (0.723) show good agreement with experimental observations shown in Fig. 4B.

crease in $[Ca^{2+}]_i$ gives rise to intercellular Ca^{2+} wave propagation presumably at the basal IP_3 level, (although the involvement of IP_3 in intercellular calcium wave propagation is not determined in our experiments and needs to be investigated.) The direct effect of PMCA inhibition is a reduced Ca^{2+} extrusion rate, which permits an increase in the diffusion range of cytosolic Ca^{2+}. Under such conditions, locally-released Ca^{2+} may diffuse without being affected by PMCA pumps and effectively sensitize IP_3Rs to further release Ca^{2+} at basal IP_3 levels. In addition, Ca^{2+} may also be effectively amplified through a phospholipase C (PLC) pathway [15], thereby enabling the propagation of a local Ca^{2+} increase in a self-amplifying manner.

The theoretical model predicts that a local Ca^{2+} increase in a non-excitable cell can propagate cell-to-cell through repetitive processes of Ca^{2+} release and diffusion when the rate of Ca^{2+} extrusion via PMCA is reduced. In addition, the theoretical model indicates that an elevated IP_3 level is not necessarily required as long as conditions are met to enable regenerative wave propagation (i.e., modifications to other parameter values can also produce self-amplifying intercellular Ca^{2+} waves). Our experimental and theoretical results together support the idea that non-excitable cells can form a highly excitable medium under the influence of a CICR-like mechanism for a range of conditions. In this way, locally sensed information can be communicated to distant cells.

Acknowledgments

The authors would like to acknowledge Dr. K. Willecke of Institut für Genetik, Germany for kindly providing HeLa Cx43 cells. This research was supported by NICT (National Institute of Communications Technology, Japan) and by NSF (National Science Foundation, USA) under Grant No. 0849358. This work was also supported by grants from the MEXT of Japan to T.H. and Y.H. Further, part of this research has been carried out at the Frontier Research Base for Global Young Researchers, Osaka University, through the program Promotion of Environmental Improvement to Enhance Young Researchers' Independence, the special coordination funds for promoting science and technology, Japan ministry of education, culture, sports, science and technology.

Appendix A. Supplementary data

Supplementary data associated with this article can be found, in the online version, at doi:10.1016/j.febslet.2009.10.032.

References

[1] Roderick, H.L., Berridge, M.J. and Bootman, M.D. (2003) Calcium-induced calcium release. Curr. Biol. 13 (11), R425.

[2] Bennett, D.L., Cheek, T.R., Berridge, M.J., De Smedt, H., Parys, J.B., Missiaen, L. and Bootman, M.D. (1996) Expression and function of ryanodine receptors in nonexcitable cells. J. Biol. Chem. 271 (11), 6356–6362.
[3] Leybaert, L. and Sanderson, M.J. (2001) Intercellular calcium signaling and flash photolysis of caged compounds. A sensitive method to evaluate gap junctional coupling. Meth. Mol. Biol. 154, 407–430.
[4] Allbritton, N.L., Meyer, T. and Stryer, L. (1992) Range of messenger action of calcium ion and inositol 1,4,5-trisphosphate. Science 258 (5089), 1812–1815.
[5] Giaume, C. and Venance, L. (1998) Intercellular calcium signaling and gap junctional communication in astrocytes. Glia 24 (1), 50–64.
[6] Leybaert, L., Paemeleire, K., Strahonja, A. and Sanderson, M.J. (1998) Inositol-trisphosphate-dependent intercellular calcium signaling in and between astrocytes and endothelial cells. Glia 24 (4), 398–407.
[7] Lajas, A.I., Sierra, V., Camello, P.J., Salido, G.M. and Pariente, J.A. (2001) Vanadate inhibits the calcium extrusion in rat pancreatic acinar cells. Cell Signal 13 (6), 451–456.
[8] Kurnellas, M.P., Nicot, A., Shull, G.E. and Elkabes, S. (2005) Plasma membrane calcium ATPase deficiency causes neuronal pathology in the spinal cord: A potential mechanism for neurodegeneration in multiple sclerosis and spinal cord injury. Faseb J. 19 (2), 298–300.
[9] Elfgang, C., Eckert, R., Lichtenberg-Frate, H., Butterweck, A., Traub, O., Klein, R.A., Hulser, D.F. and Willecke, K. (1995) Specific permeability and selective formation of gap junction channels in connexin-transfected HeLa cells. J. Cell Biol. 129 (3), 805–817.
[10] Goldbeter, A., Dupont, G. and Berridge, M.J. (1990) Minimal model for signal-induced Ca^{2+} oscillations and for their frequency encoding through protein phosphorylation. Proc. Natl. Acad. Sci. 87, 1461–1465.
[11] Wanaverbecq, N., Marsh, S.J., Qatari, M.A. and Brown, D.A. (2003) The plasma membrane calcium-ATPase as a major mechanism for intracellular calcium regulation in neurones from the rat superior cervical ganglion. J. Physiol. 550 (1), 83–101.
[12] Leite, M.F. et al. (2002) Molecular basis for pacemaker cells in epithelia. J. Biol. Chem. 277 (18), 16313–16323.
[13] Yule, D.I., Stuenkel, E. and Williams, J.A. (1996) Intercellular calcium waves in rat pancreatic acini: Mechanism of transmission. Am. J. Physiol. 271 (4 Pt 1), C1285–C1294.
[14] Zimmermann, B. and Walz, B. (1999) The mechanism mediating regenerative intercellular Ca^{2+} waves in the blowfly salivary gland. Embo J. 18 (12), 3222–3231.
[15] Tsien, R.W. and Tsien, R.Y. (1990) Calcium channels, stores, and oscillations. Annu. Rev. Cell Biol. 6, 715–760.